Role of Lone-Pair Electrons in Producing Minimum Thermal Conductivity in Nitrogen-Group Chalcogenide Compounds

Eric J. Skoug and Donald T. Morelli

Phys. Rev. Lett. **107**, 235901 — Published 30 November 2011

DOI: 10.1103/PhysRevLett.107.235901

Title: The Role of Lone-Pair Electrons in Producing Minimum Thermal Conductivity in Group VA Chalcogenide Compounds

Abstract: Fully dense crystalline solids with extremely low lattice thermal conductivity (κ_L) are of practical importance for applications including thermoelectric energy conversion and thermal barrier coatings. Here we show that lone-pair electrons can give rise to minimum κ_L in chalcogenide compounds that contain a nominally trivalent group VA element. Electrostatic repulsion between the lone-pair electrons and neighboring chalcogen ions creates anharmonicity in the lattice, the strength of which is determined by the morphology of the lone-pair orbital and the coordination number of the group VA atom.

Names of authors: Eric J. Skoug* and Donald T. Morelli

Department of Chemical Engineering and Materials Science

Michigan State University

East Lansing, MI, 48824

*Corresponding author

The transport of heat in crystalline solids has long been a topic of interest in solid-state physics. Debye first studied heat transport by lattice phonons in 1912 [1] and to this day the lattice thermal conductivity (κ_L) of a vast array of crystalline materials can be estimated, to a first approximation, using some form of the Debye model. An interesting problem arises when one encounters a material whose lattice thermal conductivity cannot be explained using conventional phonon transport theory, as in the case of an ordered crystal that exhibits "minimum thermal conductivity" (κ_{min}) behavior at ordinary temperatures. Slack first introduced this concept, which he defined as the case where all phonons are scattered so frequently that the average mean free path is on the order of one phonon wavelength [2]. It is not uncommon for κ_L of an ordered crystal to approach κ_{min} near its melting temperature due to intrinsic phonon-phonon interactions alone; however similar behavior near room temperature is quite rare and the phonon scattering mechanisms that govern such behavior are not well understood. Here we show that lone electron pairs (LEPs) can produce κ_{min} behavior in group VA chalcogenides. Our results indicate that the morphology of the LEP is directly related to lattice anharmonicity, and the propensity of a given crystal to exhibit κ_{min} behavior can be predicted based on the local atomic environment of the group VA atom. A better understanding of intrinsically limited κ_L is important to not only our fundamental picture of phonon transport in solids, but also has major implications in the design of high performance thermoelectric materials and thermal barrier coatings, which require materials with extremely low κ_L.

We have recently shown that the compounds Cu_3SbSe_4 and Cu_3SbSe_3 possess vastly different κ_L despite their similarities in average atomic mass and stoichiometry [3]. In the former compound, κ_L increases rapidly with decreasing temperature due to

vanishing phonon-phonon interactions (typical for a crystalline material), while the latter compound has a temperature independent κ_L near its minimum possible value even at cryogenic temperatures. A similar situation occurs in the case of $AgInTe_2$ versus $AgSbTe_2$, where the κ_L of the former compound is "normal" and the latter is glass-like [4 – 5]. The common thread among the compounds with anomalously low κ_L is that they contain Sb nominally in the trivalent (+3) valence state, meaning that the Sb 5s electrons are non-bonding. Petrov and Shtrum originally proposed the idea that the "lone-pair" 5s electrons could interact with the valence electrons of adjacent atoms upon thermal agitation and cause increased anharmonicity in the lattice (thus lowering κ_L) [4], a concept recently revisited by Morelli *et. al.* [5]. This provides a qualitative explanation for the low intrinsic κ_L of these compounds, but to our knowledge no direct evidence of a relationship between LEPs and low κ_L has been presented.

The Cu-Sb-Se ternary system presents a unique opportunity to study the effect of LEPs on κ_L. In addition to Cu_3SbSe_4 and Cu_3SbSe_3, the compound $CuSbSe_2$ forms readily and has a structure similar to that of Cu_3SbSe_3 (orthorhombic, space group *Pmna* [6]). Naively one would expect these three compounds to all have κ_L similar to that of Cu_3SbSe_4 since their average atomic masses are nearly the same and none of them possesses an overly complex crystal structure. The only reasonable explanation for the large κ_L discrepancy (see Figure 1) is that there must be an intrinsic phonon scattering mechanism acting with increasing strength as the composition changes from Cu_3SbSe_4 to $CuSbSe_2$ to Cu_3SbSe_3. These results are consistent with the hypothesis that the Sb 5s LEP gives rise to anharmonic forces in the lattice, but since Sb is nominally in the +3 state in both $CuSbSe_2$ and Cu_3SbSe_3 the κ_L difference between these two compounds is not

immediately clear.

In Cu_3SbSe_4, Sb is coordinated by 4 selenium atoms with ideal tetrahedral Se–Sb–Se bond angles of 109.5° [7], suggesting sp^3 hybridization of the Sb valence electron orbitals. In this case, all of the Sb valence electrons form bonds with neighboring Se atoms. In $CuSbSe_2$, however, Sb is coordinated by 3 Se atoms in a trigonal pyramidal configuration with an average Se–Sb–Se bond angle of 95.24° [6]. In this arrangement only the Sb 5p electrons form bonds with Se, leaving the Sb 5s electrons "free" to orient along the missing vertex of the tetrahedron, as defined by the valence shell electron pair repulsion (VSEPR) theory. The configuration is similar for Cu_3SbSe_3 except the average Se–Sb–Se bond angle is 99.42°, intermediate to those of the other two compounds [8]. Once again the Sb 5s LEP forms an imperfect tetrahedron with the Sb 5p bonding electrons (see Figure 2).

The coordination environment of Sb in Cu_3SbSe_4 requires little interpretation as it is analogous to the well-known group IV, III-V, and II-V semiconductors. In $CuSbSe_2$ and Cu_3SbSe_3, however, Sb has the same coordination yet the average Se–Sb–Se angle is quite different. Wang and Liebau studied this effect, and found that the change in X–Sb–X bond angle (where X denotes a chalcogen atom) correlates to the stereochemical activity of the LEP, or the delocalization of the Sb 5s LEP away from the Sb nucleus [9]. This phenomenon stems from the fact that the actual valence of Sb in a given compound is not necessarily purely trivalent or pentavalent, but rather a combination of these two extremes. For a purely pentavalent Sb compound, as in the case of Cu_3SbSe_4, all of the Sb valence electrons are completely delocalized from the Sb nucleus and form bonds that assume the ideal tetrahedral angle of 109.5°. For a purely trivalent compound the Sb 5s

electrons remain concentrated around the Sb nucleus, thereby inducing a Coulombic repulsion with the bonding Sb 5p electrons, causing the X–Sb–X bond angle to decrease. As the actual Sb valence varies from +3 to +5 the 5s LEP progressively retracts from the nucleus, weakening the repulsion and causing the bond angle to increase. Wang and Liebau compiled average X–Sb–X bond angles ($\overline{\alpha}$) from the literature and derived an expression for the effective valence of Sb^{3+} in SbX_n polyhedral [9]:

$$^{eff}V_{Sb^{3+}}(\overline{\alpha}) = 3[1 + 0.0128(\overline{\alpha} - 90)]. \quad (1)$$

The difference in Se–Sb–Se bond angle between $CuSbSe_2$ and Cu_3SbSe_3 can now be interpreted as a difference in effective Sb valence state. $^{eff}V_{Sb}{}^{3+}$ = 3.2 for $CuSbSe_2$ and 3.36 for Cu_3SbSe_3, indicating that the LEP is farther removed from the Sb nucleus in the latter compound. The main idea behind the relationship between LEPs and low κ_L is that as atoms approach one another during thermal agitation, the overlapping wave functions of the LEP and nearby valence electrons will induce a non-linear repulsive electrostatic force causing increased anharmonicity in the lattice. As the LEP moves away from the Sb nucleus, anharmonic interactions with adjacent atoms intensify and κ_L decreases. The highest degree of anharmonicity should thus be achieved when the LEP is far removed from the Sb nucleus yet not participating in bonding, intermediate to the case of Sb^{3+} ($\overline{\alpha}$ ≈ 90°) and Sb^{5+} ($\overline{\alpha}$= 109.5°). This explains the κ_L difference between the three Cu-Sb-Se compounds shown in Figure 1 and provides direct evidence in favor of a relationship between LEPs and κ_L. The acoustic mode Grüneisen parameters of Cu_3SbSe_3 and Cu_3SbSe_4, which quantify lattice anharmonicity in these compounds, have been obtained from density functional theory (DFT) calculations and are in good agreement with these results (details to follow in a forthcoming publication[10]).

If there exists a universal relationship between LEP morphology and κ_L, then it should be possible to generalize the results of the Cu-Sb-Se compounds to other group VA chalcogenides. With this in mind, a comprehensive literature review of the crystal structures and room temperature κ_L values of group VA chalcogenides was conducted. Literature data are given in Table I for compounds of the form M_2X_3 and $A_iM_jX_k$ where M = As, Sb, or Bi, X = S, Se, or Te, and A = Cu, Ag, Tl, or an alkali metal. The average X–M–X bond angles were calculated from the bond angles of the nearest neighbor M–X bonds, which form the coordination polyhedra around the M atoms.

The room temperature κ_L versus average X–M–X bond angle ($\overline{\alpha}$) of the compounds listed in Table I and plotted in Figure 3 corroborate the trend observed in the Cu-Sb-Se system. The broad minimum in κ_L lies intermediate to the smallest ($\overline{\alpha}$ = 86.5°) and largest ($\overline{\alpha}$ = 109.5°) $\overline{\alpha}$ values, where the LEP is far removed from the nucleus of the M atom without forming an M–X bond. Several of the compounds with intermediate $\overline{\alpha}$ have κ_L in the range of estimated the κ_{min} values for these compounds (indicated by the shaded region in Figure 3)[i].

Although the general trend of decreasing κ_L with increasing $\overline{\alpha}$ (for $\overline{\alpha}$ < 100°) is clearly illustrated in Figure 3 there is considerable scatter in the data, particularly for the intermediate ($\overline{\alpha}$ = 90–100°) bond angles. To better understand the influence of LEPs on κ_L we must look closer at the local atomic environment of the M atom. Figure 4 shows the data from Figure 3 (excluding the compounds with $\overline{\alpha}$ near 109.5° since they do not contain LEPs, as discussed above) plotted separately according to the coordination

[i] Refer to the supplementary information for more detail regarding κ_{min} calculations

number (CN) of the M atom, which corresponds to the number of nearest neighbor chalcogen atoms surrounding the M atom. For each CN group, κ_L decreases nearly linearly with increasing $\overline{\alpha}$, suggesting that κ_L depends on not only the morphology of the LEP, but also the nature of the MX_n polyhedra.

Figure 4 also shows that κ_L decreases more rapidly with increasing CN, as indicated by the changing slope of the line of best fit (dashed lines in Figure 4). For compounds with CN $\geq$ 6 (octahedral or greater coordination) the slope is -0.64, while for CN = 4–5 (trigonal bypyramidal-like corrdination) and CN = 3 (trigonal pyramidal coordination) it is -0.37 and -0.18 respectively. When the M atom has CN $\geq$ 6, atomic packing rules require that is it surrounded by chalcogen atoms on all sides. In this case the LEP assumes a spherical distribution around the M nucleus, and any small retraction of the LEP away from the nucleus will cause a strong repulsion with a nearby negatively charged chalcogen atom (see supplementary information for supporting arguments). The maximum X–M–X bond angle for CN = 6 is 90^o (NaCl-type structure), and all of the compounds that fall into this category have κ_L < 1.0 W/mK at room temperature.

The M atoms in compounds with CN = 4–5 have essentially octahedral coordination with 2 or 3 of the chalcogen atoms far removed from their ideal octahedral positions. In this arrangement, the LEP is retracted from the M nucleus in the direction of the missing chalcogen atom(s). The absence of a complete octahedron around the M atom results in a more gradual decrease of κ_L with $\overline{\alpha}$ due to less interaction between the LEP and surrounding chalcogen atoms. For CN = 3 the M atom is surrounded by exactly 3 chalcogen atoms in a trigonal pyramid and the LEP is retracted from the nucleus towards the missing link of the tetrahedron. The absence of nearby chalcogen atoms in this

direction means that strong lattice anharmonicity will not be achieved until the LEP is far removed from the M nucleus, and indeed low κ_L values are not observed in these compounds until $\overline{\alpha}$ > 98-100°. Similar compounds with CN = 3 and $\overline{\alpha}$ > 100° are rare but have exceedingly low κ_L, for example Tl_3AsSe_3 which has $\overline{\alpha}$ = 118° and κ_L = 0.35 W/m*K at room temperature [11 – 12].

We have demonstrated that the interaction of lone-pair electrons with neighboring atoms can produce minimum lattice thermal conductivity in group VA chalcogenide compounds. Both the morphology of the lone-pair electron orbital and the coordination environment of the group VA atom affect the extent to which the LEPs induce anharmonicity in the crystal lattice. Based on these results, the propensity of a given group VA chalcogenide compound to exhibit κ_{min} behavior can be evaluated based solely on crystallographic data. For compounds with CN ≥ 6, an X–M–X bond angles close to $\overline{\alpha}$ = 90° are preferred, whereas for CN = 4-5 and 3 $\overline{\alpha}$ should be 95-96° and >99° respectively to achieve κ_{min} behavior. These guidelines could prove useful in identifying potential new compounds for thermoelectric applications as well as thermal barrier coatings.

References

1. Zur Theorie der spezifischen Waerme, *Annalen der Physik (Leipzig)* **39**(4), p. 789 (1912)
2. Slack, G.A. Thermal conductivity of nonmetallic crystals. *Solid State Physics* **34**, 1-70 (1979).
3. Skoug, E.J., Cain, J.D., Morelli, D.T. Structural effects on the lattice thermal conductivity of ternary antimony-and-bismuth containing chalcogenide semiconductors. *Appl. Phys. Lett.* **96**, 181905 (2010).
4. Petrov, A.V. & Shtrum, E.L. Heat conductivity and the chemical bond in ABX_2-type compounds. *Soviet Physics – Solid State* **4**, 1061-1065 (1962).
5. Morelli, D.T., Jovovic, V., Heremans, J.P. Intrinsically minimal thermal conductivity in cubic I-V-VI_2 semiconductors *Phys. Rev. Lett.* **101**, 035901 (2008).
6. Zhou, J. *et. al.,* Solvothermal crystal growth of $CuSbQ_2$ (Q = S, Se) and the correlation between macroscopic morphology and microscopic structure. *Journal of Solid State Chemistry* **182**, 259-264 (2009).
7. Pfitzner, A. Crystal structure of copper tetraselenoantimonate (V), Cu_3SbSe_4. *Z. Kristallog.* **209**, 685 (1994).
8. Pfitzner, A. The Crystal Structure of Cu_3SbSe_3 (in German). *Z. Anorg. Allg. Chem.* **621**, 685-688 (1995).
9. Wang, X. & Liebau, F. Studies on bond and atomic valences. I. Correlation between bond valence and bond angles in Sb^{III} chalcogen compounds: the influence of lone-electron pairs. *Acta Cryst.* **B52**, 7-15 (1996).
10. Zhang, Y., Skoug, E., Cain, J., Wolverton, C., Morelli, D. (in preparation).
11. Hong, H. Y-P., Mikkelsen, J.C., Roland, G.W., Crystal Structure of Tl_3AsSe_3, *Mat. Res. Bull.* **9**, 365-370 (1974).
12. Ewbank, M.D., Newman, P.R., Kuwamoto, H., Thermal conductivity and specific heat of the chalcogenide salt Tl_3AsSe_3 *J. Appl. Phys.* **53**, 6450-6452 (1982).
13. Kyono, A., Kimata, M., Matsuhisa, M., Miyashita, Y., Okamoto, K. Low-temperature crystal structures of stibnite implying orbital overlap of Sb $5s^2$ inert pair electrons. *Phys. Chem. Materials* **29**, 254-260 (2002).
14. Spitzer, D.P. Lattice thermal conductivity of semiconductors: a chemical bond approach. *J. Phys. Chem. Solids* **31**, 19-40 (1970).
15. Collaboration: Authors and editors of the volumes III/17E-17F-41C: *Antimony telluride (Sb2Te3) crystal structure, chemical bond, lattice parameters (including data for Bi2Se3, Bi2Te3)*. Madelung, O., Rössler, U., Schulz, M. (ed.). SpringerMaterials - The Landolt-Börnstein Database

16. Takéuchi, Y. & Ozawa, T. The structure of $Cu_4Bi_4S_9$ and its relation to the structures of covellite, CuS and bismuthinite, Bi_2S_3. *Z. Kristallog.* **141**, 217-232 (1975).

17. Bazakutsa, V.A. & Vasil'eva, M.P. Thermal conductivity of triple semiconductors of $A^1SbC_2^6$ type as a function of chemical composition and structure. *Journal of Engineering Physics and Thermophysics* **34**, 137-140 (1978).

18. Bazakutsa, V.A., Vasil'eva, M.P., Ustimenko, V.N., Mokhir, L.M. Lattice thermal conductivity and chemical bond in the hypovalent two-cation semiconductors $A^1BC_2^6$ and $TlB^5C_2^6$. *Journal of Engineering Physics and Thermophysics* **37**, 1191-1195 (1979).

19. Kanishcheva, A.S., Kuznetsov, V.G., Lazarev, V.B., Tarasova, T.G. Crystal Structure of $RbSbS_2$. *Journal of Structural Chemistry* **18**, 849-851 (1978).

20. McCarthy, T.J. *et. al.,* Molten salt synthesis and properties of three new solid state ternary bismuth chalcogenides, β-$CsBiS_2$, γ-CsBiS2, and $K_2Bi_8Se_{13}$. *Chem. Mater.* **5**, 331-340 (1993).

21. Liang, K.S., Bienenstock, A., Bates, C.W. Structural studies of glassy $CuAsSe_2$ and Cu-As_2Se_3 alloys. *Phys. Rev. B* **10**, 1528-1538 (1974).

22. Portheine, J.C. & Nowacki, W. Refinement of the crystal structure of emplectite, $CuBiS_2$. *Z. Kristallog.* **141**, 387-402 (1975).

23. Takéuchi, Y. & Sadanaga, R. Structural principles and classification of sulfosalts. *Z. Kristallog.* **130**, 346-368 (1969).

24. Orliukas, A., Valiukenas, V., Kybartas Kezionis, A., Vilnius, V. Peculiarities of phase transitions in α and β-$AgSbS_2$ single crystals. *Ferroelectrics* **38**, 897-900 (1981).

25. Zhuze, V.P., Sergeeva, V.M., Shtrum, E.L. Semiconducting compounds with the general formula ABX_2. *Soviet Physics Technical Physics* **3**, 1925-1938 (1958).

26. Yang, Z.M. & Pertlik, F. The thallium sulfarsenites Tl_3AsS_3 and $TlAsS_2$ [thallium(I)-thioarsenates(III)]: structural characterization and syntheses. *J. Alloys Compd.* **216**, 155-158 (1994).

27. Teske, C.L. & Bensch, W. $TlBiS_2$. *Acta Cryst.* **E62**, i163-i165 (2006).

28. Olsen, A., Goodman, P., Whitfield, H.J. The structure Tl_3SbS_3, Tl_3SbSe_3, $Tl_3SbS_{3-x}Se_x$, and $Tl_3Sb_yAs_{1-y}Se_3$. *Journal of Solid State Chemistry* **60**, 305-315 (1985).

29. Chung, D.Y. *et. al.,* High thermopower and low thermal conductivity in semiconducting ternary K-Bi-Se compounds. Synthesis and properties of β-$K_2Bi_8Se_{13}$ and $K_{2.5}Bi_{8.5}Se_{14}$ and their Sb analogues. *Chem. Mater.* **9**, 3060-3071 (1997).

30. Kim, J.H. *et. al.,* Crystal growth, thermoelectric properties, and electronic structure of $AgBi_3S_5$ and $AgSb_xBi_{3-x}S_5$ (x=0.3). *Chem. Mater.* **17**, 3606-3614 (2005).

31. Berger, L.I., & Prochukhan, V.D. *Ternary Diamond-Like Semiconductors,* Consultants Bureau, New York (1969).

Acknowledgements: We thank Paul Majsztrik, Melanie Kirkham, and Edgar Lara-Curzio for helping to refine the synthesis procedure of the Cu-Sb-Se compounds; Jeffrey D. Cain for assisting in synthesis and characterization; and Dat Do, S.D. Mahanti, Yongsheng Zhang and Chris Wolverton for providing theoretical insight. This work is supported by the National Science Foundation under Award No. NSF-CBET-0754029. In addition, sample synthesis efforts were partially supported as part of the Center for Revolutionary Materials for Solid State Energy Conversion, an Energy Frontier Research Center funded by the U.S. Department of Energy, Office of Science, Office of Basic Energy Sciences under Award Number DE-SC0001054.

Figure Captions

Figure 1 – Temperature dependence of the lattice thermal conductivity (κ_L) of Cu_3SbSe_4, Cu_3SbSe_3, and $CuSbSe_2$.

Figure 2 – Schematic representation of the local atomic environment of Sb in Cu_3SbSe_4, Cu_3SbSe_3, and $CuSbSe_2$. Shaded lines represent Sb – Se bonds, dashed lines illustrate the approximate morphology of the Sb lone-pair 5s electron orbital.

Figure 3 – Room temperature lattice thermal conductivity (κ_L) versus average X – M – X bond angle ($\overline{\alpha}$) for binary and ternary group VA chalcogenides of the form M_2X_3 and $A_iM_jX_k$ where M = As, Sb, or Bi, X = S, Se, or Te, and A = Cu, Ag, Tl, or an alkali metal (see Table I for a complete list of compounds). Shaded region indicates the range of estimated κ_{min} values for the compounds in Table I.

Figure 4 – Data from Figure 3 plotted in three separate groups according to coordination number of the group VA atom. Dashed lines indicate linear approximations to the data.

Table I – Literature data for each compound plotted in Figures 3 and 4.

Compound	Crystal Structure (Space Group)	CN	$\bar{\alpha}$ (°)	κ_L at 300K	References [$\bar{\alpha}$], [κ_L]
Sb_2S_3	Orthorhombic (*Pnma*)	7	89.22	1.3	[13], [14]
Sb_2Se_3	Orthorhombic (*Pbnm*)	7	90.00	1.0	[9],[14]
Sb_2Te_3	Rhombohedral ($R\bar{3}m$)	6	88.00	2.4	[15], [14]
Bi_2S_3	Orthorhombic (Pbnm)	6	88.30	2.06	[16], [14]
Bi_2Se_3	Rhombohedral ($R\bar{3}m$)	6	86.50	2.4	[15], [14]
Bi_2Te_3	Rhombohedral ($R\bar{3}m$)	6	88.65	1.7	[15], [14]
$NaSbS_2$	Triclinic ($P\bar{1}$)	4	92.00	2.22	[9], [17]
$KSbS_2$	Monoclinic (*C2/c*)	4	92.80	1.58	[9], [18]
$KSbSe_2$	Triclinic ($P\bar{1}$)	4	93.05	1.3	[9], [17]
$RbSbS_2$	Triclinic ($P\bar{1}$)	4	91.83	1.6	[19], [17]
$CsSbS_2$	Monoclinic (*P21/c*)	3	95.02	1.2	[20], [17]
$CuAsSe_2$	Rhombohedral (*R3m*)	4	107.82	3.2	[21], [14]
$CuSbS_2$	Orthorhombic (*Pnma*)	3	95.84	1.5	[6], [14]
$CuSbSe_2$	Orthorhombic (*Pnma*)	3	95.24	1.49	[6], *
$CuBiS_2$	Orthorhombic (*Pnma*)	5	96.13	0.5	[22], [14]
$AgSbS_2$	Monoclinic (*C121*)	5	94.85	0.49	[23], [14]
$AgSbS_2$	Cubic (*Fm3m)*	6	90.00	0.402	[24], *
$AgSbSe_2$	Cubic (*Fm3m)*	6	90.0	0.77	[25], [14]
$AgSbTe_2$	Cubic (*Fm3m)*	6	90.00	0.68	[25], [5]
$AgBiSe_2$	Cubic (*Fm3m)*	6	90.00	0.62	[25], [5]
$TlAsS_2$	Monoclinic (*P21/a*)	3	99.17	0.95	[26], [18]
$TlSbS_2$	Triclinic (*P1*)	4	93.50	1.2	[9], [18]
$TlBiS_2$	Rhombohedral ($R\bar{3}m$)	6	90.00	0.875	[27], [18]
Cu_3AsS_3	Orthorhombic (*Pnma*)	3	98.37	1.1	[23], [14]
Cu_3SbSe_3	Orthorhombic (*Pnma*)	3	99.42	0.49	[8], *
Tl_3SbS_3	Rhombohedral (*R3m*)	3	99.20	0.42	[28], [14]
$K_2Bi_8Se_{13}$	Triclinic ($P\bar{1}$)	6	86.83	3.1	[20], [29]
β-$K_2Bi_8Se_{13}$	Monoclinic (*P21/m*)	6	89.05	1.28	[29]
$AgBi_3S_5$	Monoclinic (*C2/m*)	6	89.08	1.2	[30]
Cu_3AsS_4	Orthorhombic (*Pmn21)*	4	109.50	3.02	[31]
Cu_3SbS_4	Tetragonal ($I\bar{4}2m$)	4	109.50	2.7	[31], [14]
Cu_3AsSe_4	Cubic (*Pm3m*)	4	109.50	2.7	[31]
Cu_3SbSe_4	Tetragonal ($I\bar{4}2m$)	4	109.50	2.9	[7], *

*Indicates that κ_L was measured as a part of this work. Refer to supplementary information for details regarding sample synthesis and characterization.

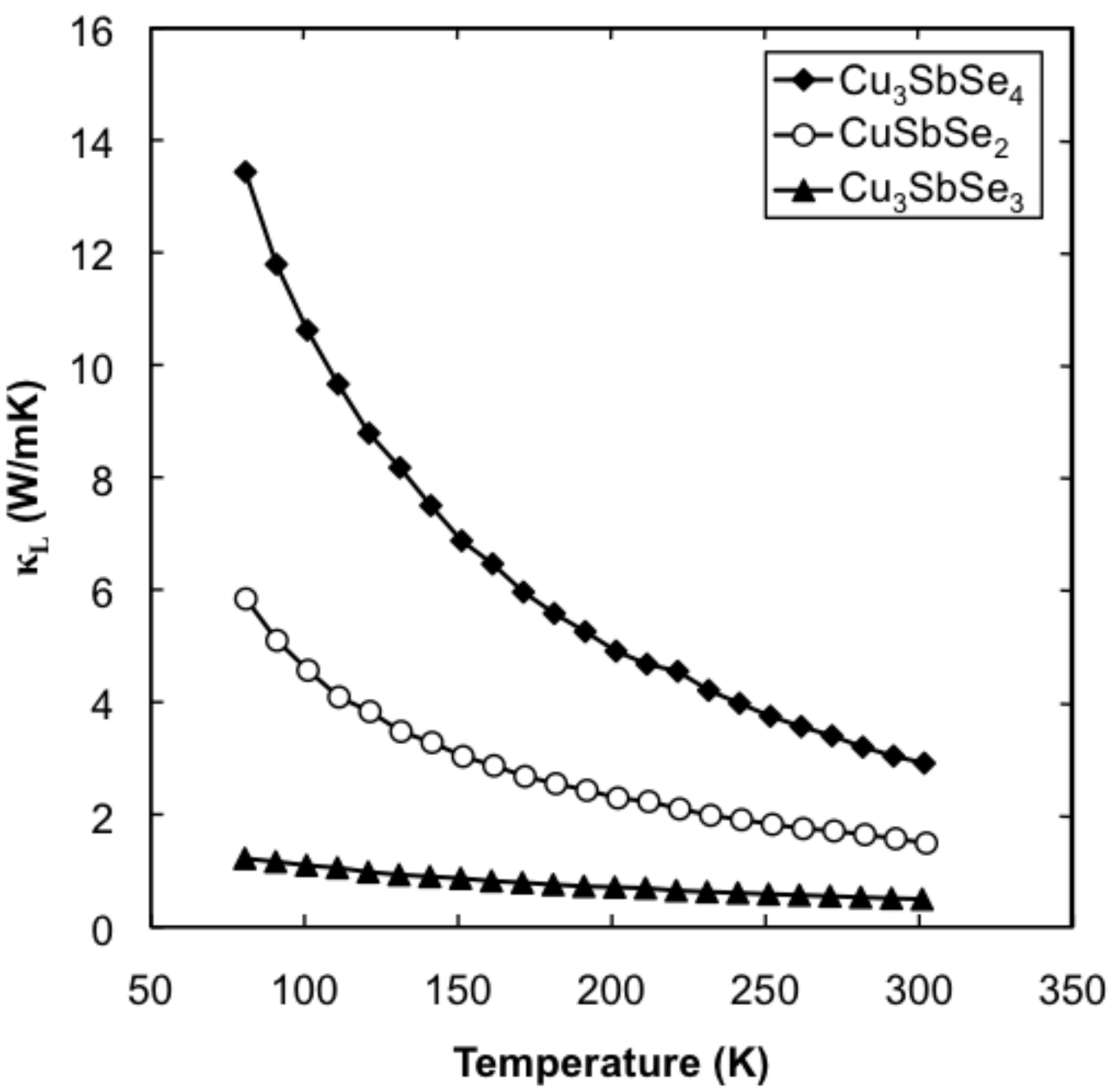
16
14
12
10
8
6
4
2
0
50
100
150
200
250
300
350
κL (W/mK)
Temperature (K)
Cu3SbSe4
CuSbSe2
Cu3SbSe3

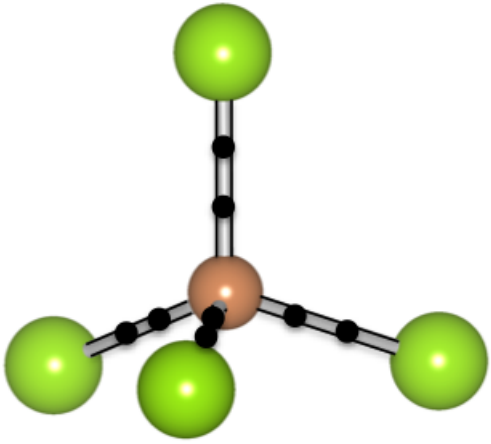

Cu_3SbSe_4

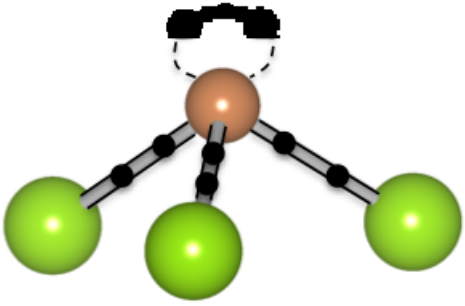

$CuSbSe_2$

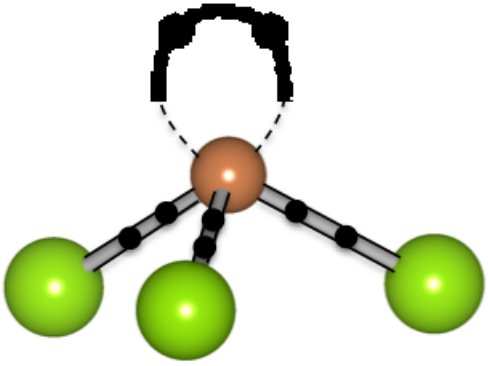

Cu_3SbSe_3

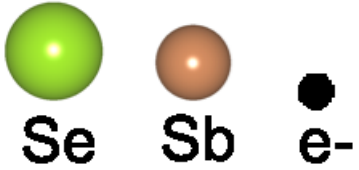

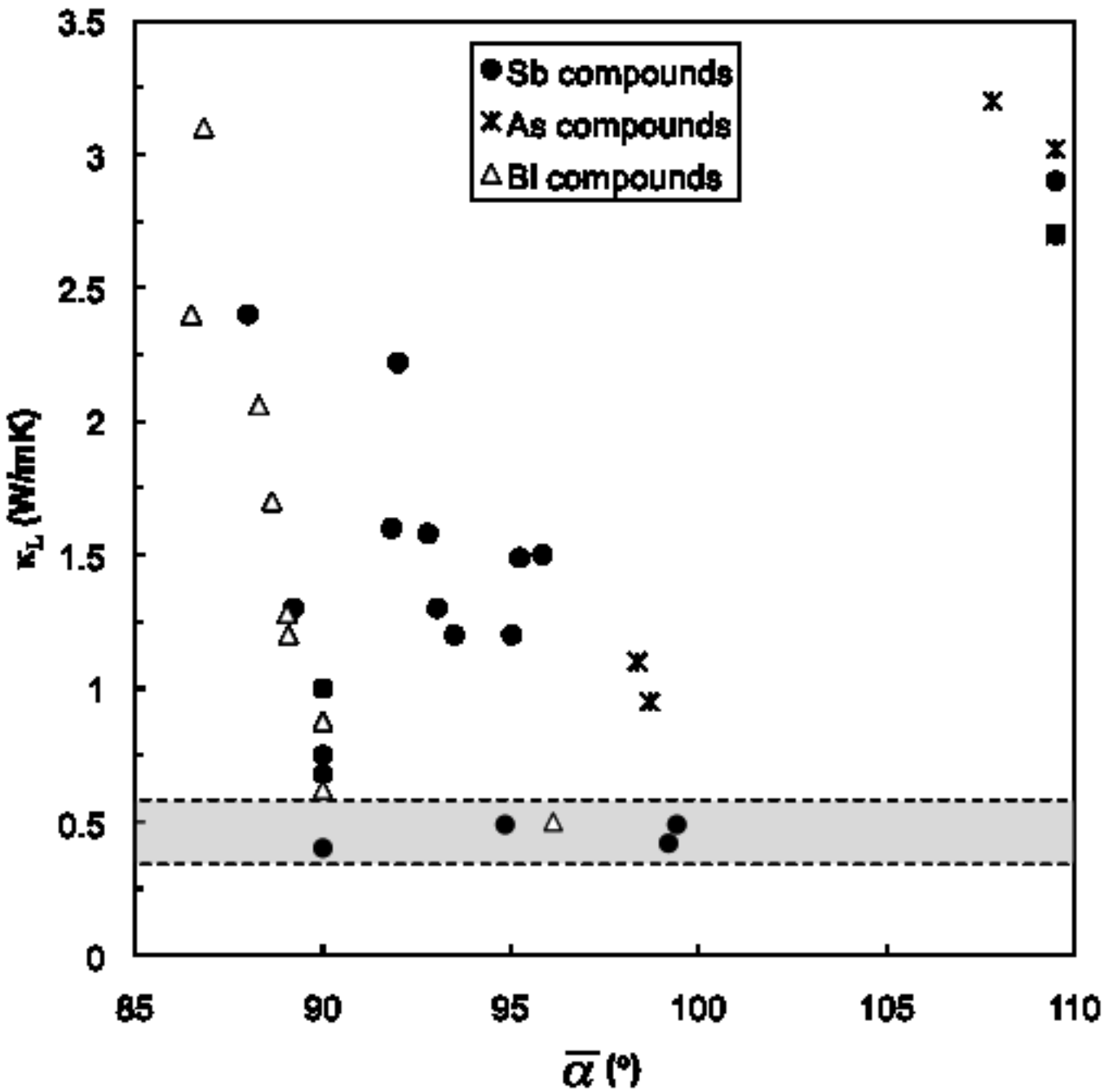
Sb compounds
As compounds
Bi compounds
κ_L (W/mK)
$\overline{\alpha}$ (°)
3.5
3
2.5
2
1.5
1
0.5
0
85
90
95
100
105
110

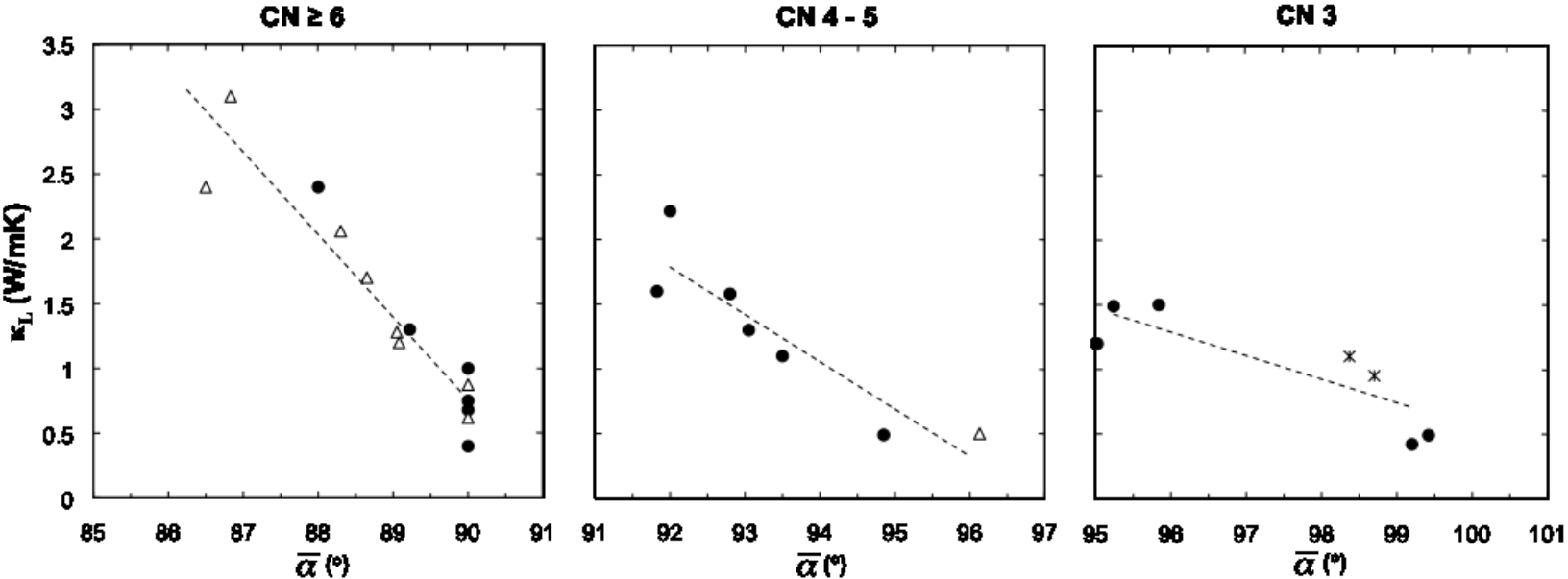
CN ≥ 6
CN 4 - 5
CN 3
κL (W/mK)
3.5
3
2.5
2
1.5
1
0.5
0
85
86
87
88
89
90
91
92
93
94
95
96
97
98
99
100
101
ᾱ (°)
ᾱ (°)
ᾱ (°)